IEEE Photonics Journal
An IEEE Photonics Society Publication

Open Access

Monolithically Integrated Dual-Wavelength Distributed Bragg Reflector Laser Photonic Integrated Circuit Chip for Continuous-Wave Terahertz Generation

Volume 13, Number 2, April 2021

Qianwen Guo
Mengdie Sun
Ruoyun Yao
Qiulu Yang
Dan Lu
Ronald Broeke
Chen Ji
Wanshu Xiong

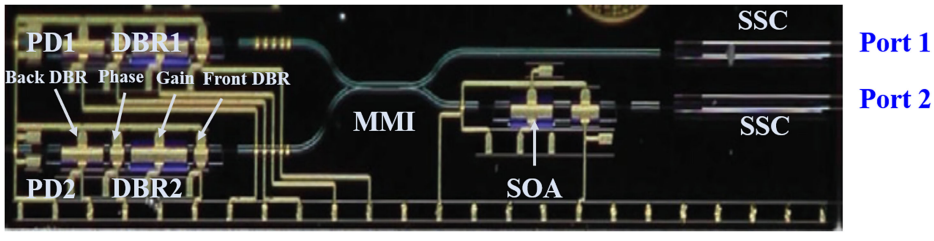

Optical microscope view of the fabricated monolithically integrated THz PIC chip

DOI: 10.1109/JPHOT.2021.3062835

Monolithically Integrated Dual-Wavelength Distributed Bragg Reflector Laser Photonic Integrated Circuit Chip for Continuous-Wave Terahertz Generation

Qianwen Guo,[1] **Mengdie Sun**,[2] **Ruoyun Yao**,[1] **Qiulu Yang**,[2] **Dan Lu**,[2] **Ronald Broeke**,[3] **Chen Ji**,[1] **and Wanshu Xiong**[1]

[1]College of Information Science and Electronic Engineering, Zhejiang University, Hangzhou 310027, China
[2]Key Laboratory of Semiconductor Material Science, Institute of Semiconductors, Chinese Academy of Sciences, Beijing 100049, China
[3]Bright Photonics, 3604 Maarssen, The Netherlands

DOI:10.1109/JPHOT.2021.3062835

Manuscript received January 28, 2021; revised February 24, 2021; accepted February 25, 2021. Date of publication March 8, 2021; date of current version March 19, 2021. This work was supported in part by National key research & development (R&D) plan 2019YFB2203801, in part by Zhejiang Lab Grant 2020LC0AD01, and in part by the National Science Foundation of China under Grant 61974132. *(Qianwen Guo and Mengdie Sun are co-first authors.)* Corresponding author: Wanshu Xiong (e-mail: xiongwanshu@zju.edu.cn).

Abstract: We report the design, fabrication and characterization of a 1.55-μm dual-wavelength Distributed Bragg Reflector (DBR) laser photonic integrated circuit (PIC) chip for continuous-waves (CW) terahertz generation. The PIC chip consists of a pair of parallel DBR lasers with integrated semiconductor optical amplifiers (SOA), and a multimode interference (MMI) coupler for combining the two wavelength channels into a single output waveguide. A room temperature continuous wave THz tuning range of 0.06 THz – 0.71 THz was obtained through optical heterodyne technique.

Index Terms: Terahertz (THz) sources, distributed Bragg reflector (DBR) lasers, monolithic integration, heterodyning, mode-beating.

1. Introduction

Technologies for the generation of electromagnetic radiations operating in the Terahertz (THz) have been developing at a rapid pace over the past two decades, overcoming the traditional challenges of the "Terahertz Gap", due to a broad range of emerging applications in THz sensing, THz spectroscopy, THz imaging, nondestructive material inspections, and THz wireless data communications [1]–[5]. In recent years, metamaterial based THz devices were also investigated for THz sensing and imaging applications, but they are still relatively novel and immature technologies not ready for commercial [6], [7]. Overall THz wave radiation can be generated by either photonics or electronics-based approaches. Electronic approaches are typically limited by the requirement of bulky and expensive equipment, tend to operate at a fixed THz signal frequency with low efficiency,

and lacking the ability for room temperature continuous frequency tuning that is a key requirement for many THz applications.

Optical heterodyning, a photonic based process, provides a simple and efficient technique for generating broadly tunable THz wave radiation at room temperature. In this approach, the output from two single wavelength lasers operating at slightly offset wavelengths are combined and coupled into a broadband photo-mixer or through nonlinear crystal based conversion process, and generating the THz radiation signal at a frequency equivalent to the wavelength difference of the two single mode laser signals [8].

While optical heterodyne experiments traditionally use two separate external solid laser sources, in recent years, THz generation by the optical heterodyning method based on dual-mode semiconductor lasers [9]–[15] attracts researchers' attention for its unique advantages such as low cost, wide continuous tuning range, room temperature operation, and the potentials for monolithic integration resulting in a very compact form factor chip solution that can be volume manufactured through standard semiconductor processing technologies. Based on the monolithic photonic integration chip (PIC) technology, various photonic components such as laser light sources, optical waveguides, optical amplifiers, and optical couplers can be monolithically integrated on the same semiconductor substrate. Therefore, the PIC technology has been recognized as one of the best technical approaches for reducing the size and cost of the devices, as well as improving the system long term reliability. Integrated tunable optical heterodyning source based on two parallel single-mode DFB lasers have been reported by several groups [16]–[20], with wavelength tuning achieved through either thermal tuning which is a relatively slow process [19], or wavelength shift through DFB section current injection which also affects the output power level [18], [20].

In this paper, we have demonstrated a monolithic 1.55-μm dual-wavelength optical heterodyne PIC chip for THz generation, integrating two DBR lasers, semiconductor optical amplifiers (SOAs), and a multimode interference (MMI) coupler on the same InP-based substrate. In principle, optical heterodyning by two DBR lasers is capable of faster frequency tuning and broader tuning range compared with the DFB laser-based solution, while maintaining constant output power which is important for optical heterodyning efficiency [21]. We report THz wave generation with a record room temperature continuous tuning range from 0.06 THz to 0.71 THz for a dual DBR monolithic PIC chip, demonstrating the potentials of our PIC chip for future high-volume and low-cost THz applications.

2. Device Design and Fabrication

Fig. 1 shows the schematic diagram of the 1.55-μm dual-wavelengths heterodyne THz PIC chip. The design and fabrication of this chip were carried out in a multi-project wafer (MPW) run on the Joint European Platform for Photonic Integration of Components and Circuits (JePPIX) InP foundry process [22]. The chip consists of multiple building blocks (BBs), which includes two DBR laser sections (DBR1 and DBR2), a 2 $\times$ 2 multimode interference coupler combining the output power from the two DBR laser sections to two separate output waveguides. A 300-μm long SOA section was integrated onto one output arm of the MMI in order to amplify the output signal and compensating for the 3dB loss at MMI combiner. The other MMI output was unamplified as a reference. The two MMI output waveguides connect to two spot-size converters (SSCs) in order to improve coupling efficiency to external lensed fibers. The total length of each DBR laser section is 900-μm, including a 300-μm back and a 100-μm front grating sandwiching a 100-μm phase section and a 400-μm gain section. The reflectivity of the front and back grating was designed to be 0.5 and 0.95, respectively, resulting in maximizing the DBR laser output emitting primarily in the front direction.

The two monitor PDs placed at the end of the back grating sections were employed to monitor output power from the back grating section and also absorbing back emitting light output, thereby eliminating any potential back reflections into the cavity, which could cause the instability in laser operation. The front and rear facets were coated with the anti-reflective (AR) coating to keep the reflection below 2E-3. As shown in Fig. 1(b), metal interconnects lines provide electrical connection

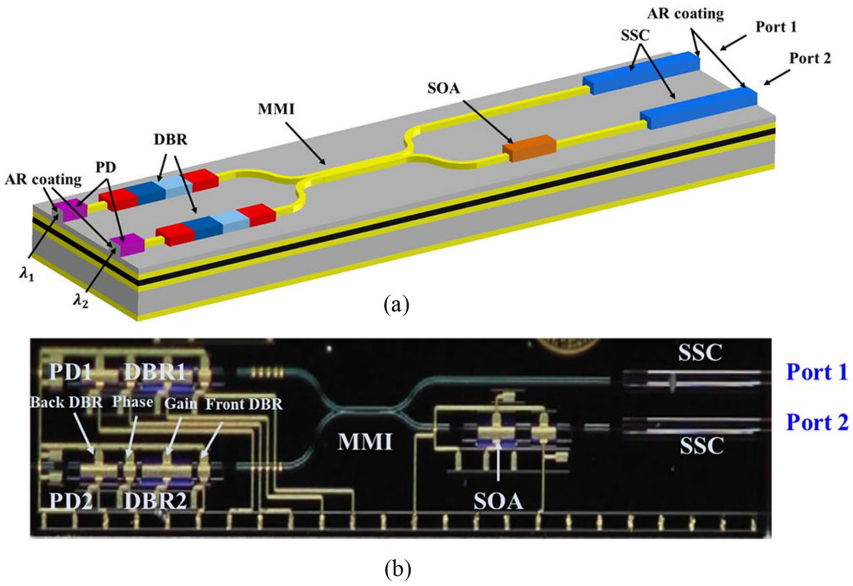

Fig. 1. (a) Schematic diagram of the 1.55 μm-dual DBR optical heterodyne THz PIC chip. (b) optical microscope view of the fabricated monolithically integrated THz PIC chip.

from various PIC chip biasing sections to the bondpad arrays at the edge of the chip, which can be probe with a custom designed DC probe card. The overall dimension of the PIC chip is 6 mm $\times$ 1.2 mm.

The fabricated PIC chip was mounted onto a ceramic submount and temperature stabilized at 20 °C using a thermoelectric cooler (TEC). In our test, the SOA amplified optical signal from port2 in Fig. 1 was coupled out into a lensed fiber, and after further amplification with an EDFA, routes to an optical spectrum analyzer (OSA) for optical spectrum, an autocorrelator for time domain optical waveform measurement, and a commercial Uni-Traveling Carrier Photodiode (UTC-PD) with integrated THz antenna for direct THz emission measurement.

3. Results and Discussions

Fig. 2(a) and (b) show the typical light-current (L-I) characteristics of the two parallel DBR lasers from our PIC chip, respectively. Each trace corresponds to a combined grating tuning current injected into the front and back DBR grating sections. Current injection into the grating section of each DBR section produces a blue-shift in the operating wavelength through plasma effect by modifying the carrier density and correspondingly the refractive index [23]. To simplify the DBR laser tuning operation, the front and back grating sections are shorted together electrically and current biasing applied using the same current source. In this approach, the grating current density remained the same, resulting in the same refractive index and Bragg wavelength shift for both the front and back grating sections. Fig. 2 shows that to first order, the DBR laser slope efficiency and output power level is independent of the grating tuning current which only shifts the DBR Bragg wavelength, as expected. The lasing threshold currents of two DBR lasers were 34 mA and 35 mA, respectively. The kink in LI curves at high gain current setting in the 80-90 mA range in Fig. 2(b) is most likely due to foundry process variation induced mode instability and mode hopping effects occurring at high optical power conditions. We carefully avoided these unstable operating regimes in our THz generation experiment. Due to the instability of the foundry process, the 300 μm SOA did not operate properly resulting in the low output power observed. We believe that it is not a major

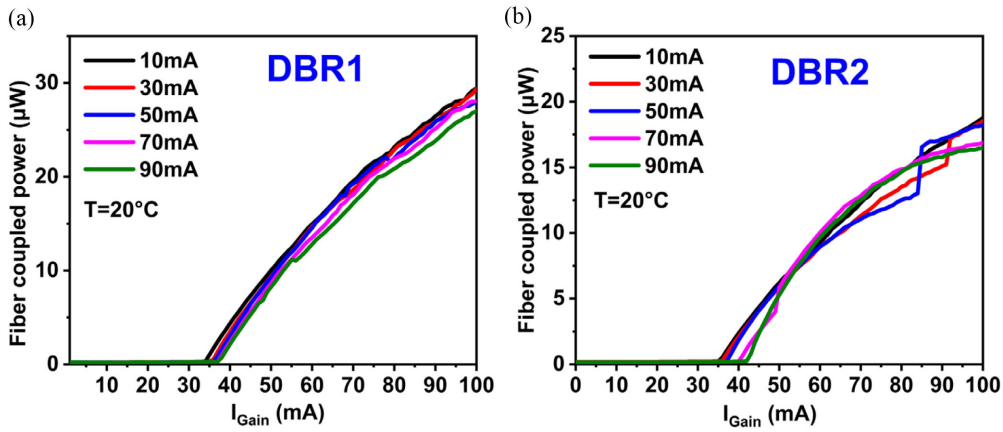

Fig. 2. L-I characteristics of the two DBR sections of the optical heterodyne PIC chip measured from output Port2. Measured fiber-coupled power as a function of applied gain section current for various DBR grating tuning current. (a) DBR1. (b) DBR2. The grating section tuning current is varied from 10 to 90 mA and the operation temperature is set to 20 °C.

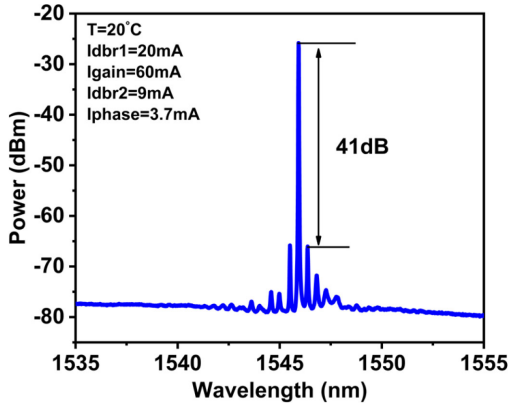

Fig. 3. A typical CW optical spectrum of a DBR laser section.

factor in evaluating THz wave generation of our prototype design, and follow up fabrication runs are ongoing which should result in much improved optical power level.

Fig. 3 shows a typical CW optical spectrum of a DBR section of the PIC chip. The injection current levels of the front and back grating sections were set at 21 mA and 7 mA respectively, the phase section injection current was 3.7 mA and the gain section biasing current was 60 mA. Under this operation condition, the center wavelength of the DBR laser was 1554.92 nm, and a high Side-mode Suppression Ratio (SMSR) of 41 dB was obtained.

Fig. 4 shows the wavelength tuning operation of the two DBR sections of a typical THz PIC chip. The initial lasing wavelengths of two DBR laser sections were 1550.8 nm (DBR1) and 1547.5 nm (DBR2), respectively. Fig. 4(a) shows the DBR1 lasing wavelength blue-shifted by 2.8 nm, with the grating tuning current varied from 0 to 100 mA, and the gain current kept constant at 50 mA. Discontinuities in the wavelength sweep can be observed, which was referred to as mode hop tuning [24], a typical feature of a DBR laser. Meanwhile, when the injection current was greater than 80 mA, the DBR wavelength blue-shift effect was replaced by a slight red-shift red. This can be explained by thermal effect at high injection current levels acting opposing the carrier plasma effect. Fig. 4(b) shows the optical spectra of DBR1 laser under different grating current biasing.

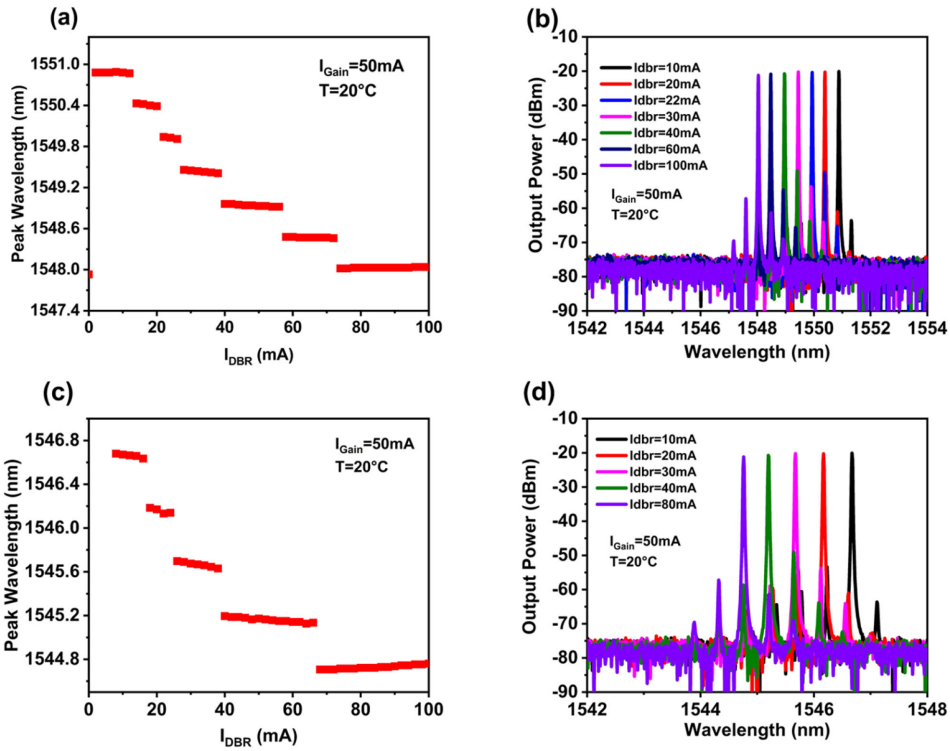

Fig. 4. Wavelength tuning operation of a two DBR THz PIC chip. (a) Lasing wavelength shift as the DBR1 grating current is tuned, with the gain section current fixed at 50 mA (b) corresponding optical spectra at different grating tuning current. (c) Lasing wavelength shift as the DBR2 grating is tuned, with the gain section current fixed at 50 mA (d) corresponding optical spectra at different grating tuning current.

Between mode hopping, single mode lasing operation with SMSR>40 dB was maintained, and optical power level remains constant as well. The DBR2 laser section of the same test PIC devices shows similar tuning characteristics as shown in Fig. 4(c) and (d). The DBR2 laser wavelength has an overall tuning range of 2.7 nm with grating current varying between 0 to 100 mA keeping the gain section constant at 50 mA. Similar to DBR1, slight red-shift can also be observed from device heating when the injection current was greater than 60 mA. Between mode hopping, DBR2 operated single mode with SMSR above 40 dB.

By adjusting the grating and phase section current of the DBR laser simultaneously, continuous wavelength tuning over a broad range can be achieved. The dependence of lasing wavelength on the phase section current tuning is shown in Fig. 5(a). Current injection into the phase section causes a local carrier density change, which in term changes the refractive index of the phase section, $\widetilde{n_p}$, changes due to the plasma effect [25]. This changes the effective cavity length, and shifts the cavity longitudinal mode resonance wavelength. Thus, by applying a combination of tuning currents to the grating and phase sections of a DBR, a broad range of continuous wavelength tuning can be achieved without experiencing mode hopping effect [26],[27]. In Fig. 5(a), the DBR2 lasing wavelength changed continuously as the phase section injection current increased, between two grating section current settings of 40 mA and 68 mA respectively, while holding the gain section current constant at 50 mA. Fig. 5(b) shows the DBR2 optical spectra when the phase current varied from 0 to 20 mA. Similar broad continuous wavelength tuning without mode hopping can be achieved in the DBR1 laser by adjusting the grating and phase section current simultaneously.

The optical spectra of the PIC chip were measured from output port2 under different tuning conditions as shown in Fig. 6 (a). The lasing wavelength of DBR1 laser can be varied from

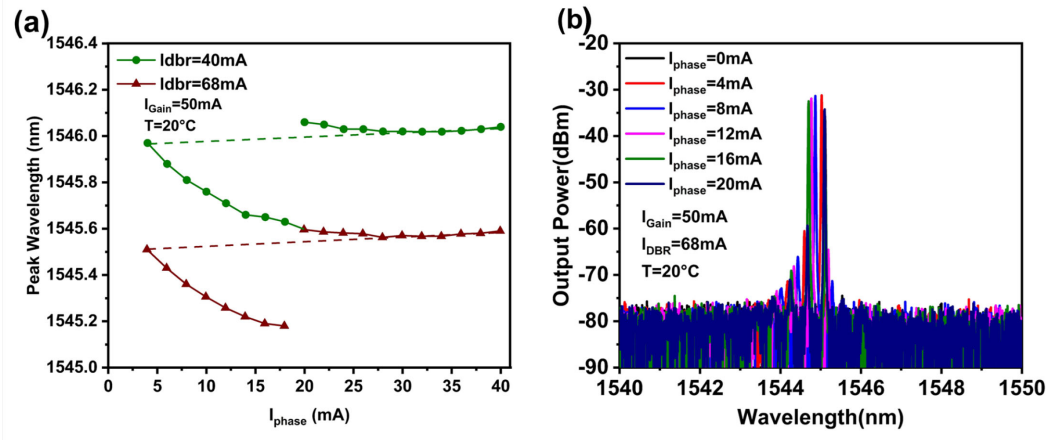

Fig. 5. Two section DBR THz PIC chip continuous wavelength tuning. (a) lasing wavelength shift as the DBR2 phase and grating current varied. (b) continuous tuning optical spectra of DBR2.

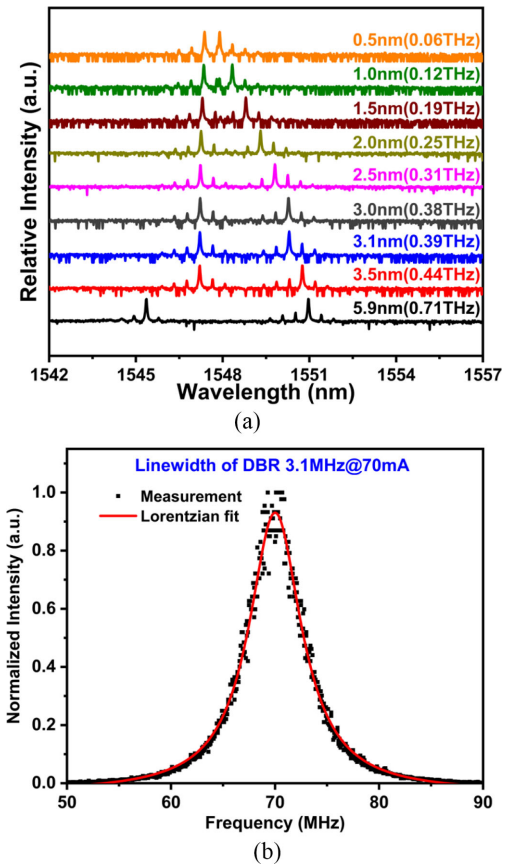

Fig. 6. (a) PIC chip optical spectrum under different tuning condition (b). Measured DBR section optical linewidth at 70mA gain biasing, fitted with a Lorentzian lineshape function.

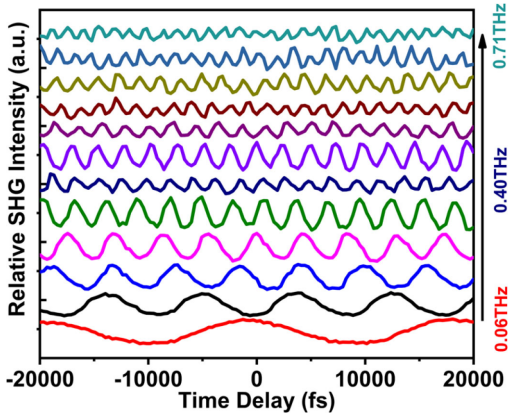

Fig. 7. Measured time domain autocorrelation traces for the two section DBR THz PIC chip, with optical heterodyne mode beating frequency continuously tunable from 0.06 THz to 0.71 THz.

1548.0 nm to 1550.8 nm, while the DBR2 laser varied from 1544.9 nm to 1547.5 nm. Accordingly, the wavelength separation between two DBR lasing modes can be continuously tuned from 0.5 nm to 5.9 nm, corresponding to an optical heterodyne mode-beating frequency ranging from 0.06 THz to 0.71 THz at 1550 nm. Meanwhile, each DBR laser section operated with a stable single-mode output and maintained high spectral purity with a SMSR greater than 40 dB throughout the tuning range. The actual optical linewidth of the DBR laser sections was measured using a delayed self heterodyne method, and shows a measured value of a few MHz over a broad range of DBR gain section current level. Fig. 6 (b) shows a typical DBR linewidth measurement result of 3.1 MHz at 70 mA gain section biasing current, fitted with a Lorentzian lineshape function. For demonstration of the optical heterodyne effect [8], Fig. 7 shows the autocorrelation measurement of the dual DBR laser output measured at output port2. Stable and sinusoidal autocorrelation traces are obtained, with the beating signal frequency continuously tunable from 0.06 THz to 0.71 THz by current injection tuning. This result is also consistent with the corresponding optical spectral results shown in Fig. 6, and shows that the two DBR sections monolithically integrated onto the same InP PIC chip has enough sufficient coherence to for THz signal generation.

The dual DBR optical heterodyne PIC output signal after EDFA amplification was coupled into a commercial UTC-PD detector with integrated antenna, the generated THz emission signal was then focused with a Si lens into a Golay cell for direct THz emission power measurement. The UTC-PD biasing voltage was set at -1.0 V, with an observed DC monitor photocurrent level of 1.6 mA. Fig. 8 shows the measured THz emission power vs the optical heterodyne frequency equal to the wavelength difference between the two DBR channels, under the same PIC biasing conditions as in Fig. 7. Continuously tunable THz emission from 0.06 to 0.71 THz can be directly observed, matching the autocorrelation result in Fig. 7, further demonstrating the optical heterodyne THz generation capacity of our PIC chip. The fast rise in the THz signal strength near 0.1 THz and subsequent roll-off toward higher frequency can be attributed to the intrinsic frequency response of the UTC-PD detector.

4. Conclusion

In this paper, we have reported a monolithic 1.55-μm dual-wavelength DBR laser PIC chip for the first time with an integrated MMI combiner for widely tunable optical heterodyne THz generation. A room temperature continuous frequency tuning ranging from 0.06 THz to 0.71 THz (0.5 nm–5.9 nm wavelength tuning) has been demonstrated, and confirmed by autocorrelation and direct THz emission measurements. The dual-wavelength DBR PIC design is expected to deliver a wider and more efficient frequency tuning compared with other reported approaches such as the dual

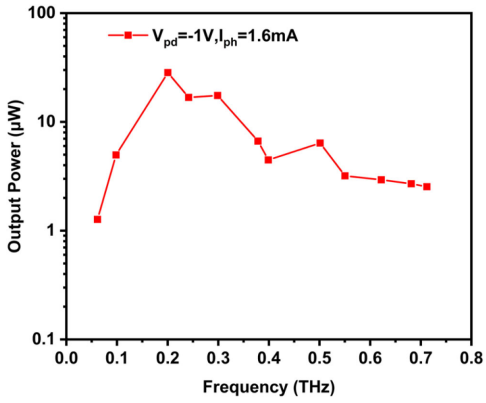

Fig. 8. Continuously tunable dual DBR PIC chip optical heterodyne direct THz emission from 0.06 to 0.71 THz, measured using a commercial UTC-PD and Golay cell.

DFB designs. Overall our monolithic PIC chip design provides a commercially viable low cost, compact size, reliable and volume manufacturable THz light source solution for a broad range of THz sensing and communication applications.

References

[1] Tonouchi and Masayoshi, "Cutting-edge terahertz technology," *Nat. Photon.*, vol. 1, no. 2, pp. 97–105, 2007.
[2] I. F. Akyildiz, J. M. Jornet, and C. Han, "Terahertz band: Next frontier for wireless communications," *Phys. Commun.*, vol. 12, no. sep., pp. 16–32, 2014.
[3] T. Robin, C. Bouye, and J. Cochard, "Terahertz applications: Trends and challenges," *Proc. SPIE - Int. Soc. Opt. Eng.*, vol. 8985, 2014.
[4] D. Saeedkia and S. Safavi-Naeini, "Terahertz photonics: Optoelectronic techniques for generation and detection of terahertz waves," *J. Lightw. Technol.*, vol. 26, no. 15, pp. 2409–2423, 2008.
[5] P. Shumyatsky and R. R. Alfano, "Terahertz sources," *J. Biomed. Opt.*, vol. 16, no. 3, 2011, Art. no. 033001.
[6] Z. Shen*et al.*, "Liquid crystal integrated metalens with tunable chromatic aberration," *Adv. Photon.*, vol. 2, no. 3, 2020, Art. no. 036002.
[7] R. Singh, W. Cao, I. Al-Naib, L. Cong, W. Withayachumnankul, and W. Zhang, "Ultrasensitive terahertz sensing with high-Q fano resonances in metasurfaces," *Appl. Phys. Lett.*, vol. 105, no. 17, 2014, Art. no. 171101.
[8] O. Acef, F. Nez, and G. Rovera, "Optical heterodyning with a frequency difference of 1 THz in the 850-nm range," *Opt. Lett.*, vol. 19, no. 17, pp. 1275–1277, 1994.
[9] A. Klehr *et al.*, "High-Power monolithic two-mode DFB laser diodes for the generation of THz radiation," *IEEE J. Sel. Topics Quantum Electron.*, vol. 14, no. 2, pp. 289–294, Apr. 2008.
[10] L. Hou, M. Haji, I. Eddie, H. Zhu, and J. H. Marsh, "Laterally coupled dual-grating distributed feedback lasers for generating mode-beat terahertz signals," *Opt. Lett.*, vol. 40, no. 2, pp. 182–185, 2015.
[11] H. Shao *et al.*, "Heterogeneously integrated III–V/silicon dual-mode distributed feedback laser array for terahertz generation," *Opt. Lett.*, vol. 39, no. 22, pp. 6403–6406, 2014.
[12] G. Carpintero, S. Hisatake, D. de Felipe, R. Guzman, T. Nagatsuma, and N. Keil, "Wireless data transmission at terahertz carrier waves generated from a hybrid inp-polymer dual tunable DBR laser photonic integrated circuit," *Sci. Rep.*, vol. 8, no. 1, pp. 1–7, 2018.
[13] J. O. Gwaro, C. Brenner, B. Sumpf, A. Klehr, J. Fricke, and M. R. Hofmann, "Terahertz frequency generation with monolithically integrated dual wavelength distributed Bragg reflector semiconductor laser diode," *IET Optoelectron.*, vol. 11, no. 2, pp. 49–52, 2017.
[14] Y. Liu *et al.*, "Dual-wavelength DBR laser integrated with high-speed EAM for THz communications," *Opt. Exp.*, vol. 28, no. 7, pp. 10542–10551, 2020.
[15] K. Nallappan, H. Guerboukha, C. Nerguizian, and M. Skorobogatiy, "Live streaming of uncompressed HD and 4K videos using terahertz wireless links," *IEEE Access*, vol. 6, pp. 58030–58042, Oct. 2018.
[16] M. Theurer *et al.*, "Photonic-integrated circuit for continuous-wave THz generation," *Opt. Lett.*, vol. 38, no. 19, pp. 3724–3726, 2013.
[17] F. Van Dijk *et al.*, "Integrated InP heterodyne millimeter wave transmitter," *IEEE Photon. Technol. Lett.*, vol. 26, no. 10, pp. 965–968, May 2014.
[18] M. Sun *et al.*, "Integrated four-wavelength DFB diode laser array for continuous-wave THZ generation," *IEEE Photon. J.*, vol. 8, no. 4, Jun. 2016, Art. no. 1502508.
[19] N. Kim *et al.*, "Tunable continuous-wave terahertz generation/detection with compact 1.55 μm detuned dual-mode laser diode and ingaas based photomixer," *Opt. Exp.*, vol. 19, no. 16, pp. 15397–15403, 2011.

[20] M. Sun *et al.*, "Continuously tunable terahertz signal generation with an integrated 1.55-μm dual-wavelength DFB photonic chip," in *Proc. IEEE Photon. Conf. (IPC)*, 2016, pp. 228–229.
[21] P. An, E. A. Bente, and M. J. Heck, "High-power continuously tunable terahertz beat note generation based on a generic photonic integration platform," in *Proc. Conf. Lasers Electro-Opt. (CLEO)*, 2020, pp. 1–2.
[22] Joint European Platform for Photonic Integration of Components and Circuits (JePPIX), [Online]. Available: www.JePPIX.eu
[23] B. R. Bennett, R. A. Soref, and J. A. Del Alamo, "Carrier-induced change in refractive index of InP, GaAs and InGaAsP," *IEEE J. Quantum Electron.*, vol. 26, no. 1, pp. 113–122, Jan. 1990.
[24] Y. Liu, P. Davis, and T. Aida, "Synchronized chaotic mode hopping in DBR lasers with delayed opto-electric feedback," *IEEE J. Quantum Electron.*, vol. 37, no. 3, pp. 337–352, Mar. 2001.
[25] A. Tsigopoulos, T. Sphicopoulos, I. Orfanos, and S. Pantelis, "Wavelength tuning analysis and spectral characteristics of three-section DBR lasers," *IEEE J. Quantum Electron.*, vol. 28, no. 2, pp. 415–426, Feb. 1992.
[26] M. Teshima, "Dynamic wavelength tuning characteristics of the 1.5-/spl mu/m three-section DBR lasers: Analysis and experiment," *IEEE J. Quantum Electron.*, vol. 31, no. 8, pp. 1389–1400, Aug. 1995.
[27] B. Mason, G. A. Fish, S. P. DenBaars, and L. A. Coldren, "Widely tunable sampled grating DBR laser with integrated electroabsorption modulator," *IEEE Photon. Technol. Lett.*, vol. 11, no. 6, pp. 638–640, Jun. 1999.